



Letters

A Soft-Switching Non-Inverting Buck–Boost Converter With Efficiency and Performance Improvement

Yong Zhang , Member, IEEE, Xu-Feng Cheng , and Chengliang Yin 

Abstract—This letter proposed a new soft-switching non-inverting buck–boost converter (NIBBC) by introducing the magnetic coupling effect to an existing soft-switching dc/dc converter. The new NIBBC obtains two superiorities: one magnetic core is removed to improve the efficiency; the magnetic coupling effect can give an adjustable soft-switching range. Operating principles and converter characteristics of the new NIBBC are presented. An experimental prototype of the new NIBBC is built, and switching waveforms and the efficiency are measured. Experimental results show that the new NIBBC can obtain soft-switching conditions and has efficiency improvement comparing to hard-switching converter and another soft-switching dc/dc converter.

Index Terms—Coupled inductor, dc/dc converter, non-inverting buck-boost converter, soft-switching.

I. INTRODUCTION

RECENT years, the soft-switching technology of the non-inverting buck–boost converter (NIBBC) gets attention from some researchers. Due to the existing of four switches and incomplete current output, the efficiency of NIBBC is lower than the traditional bidirectional buck/boost converter. The use of soft-switching methods can improve the efficiency of NIBBCs. Then, the NIBBC can obtain the practical value. Based on the use of auxiliary circuits and auxiliary switches (AS), the soft-switching technology of NIBBCs can be divided into three types: none auxiliary circuits (NAC) NIBBCs [1], [2], passive auxiliary circuits (PAC) NIBBCs [3]–[5], and AS NIBBCs [6].

The simplest soft-switching method is NAC NIBBCs. This method uses triangular current mode operation and corresponding modulation method to provide soft-switching conditions for NIBBCs without using any auxiliary circuits [1], [2], [7]. However, large current ripples in this method will reduce the efficiency improvement effect. Auxiliary circuits without switches are used in PAC NIBBCs to obtain soft-switching conditions [3]–[5]. A coupled inductor, two small inductors, and two power

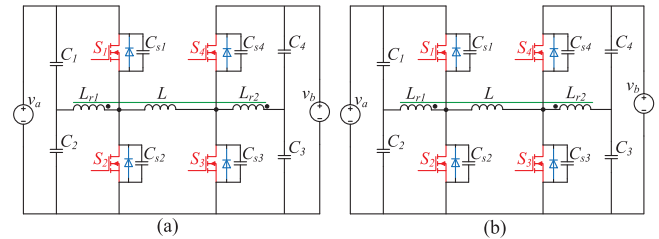


Fig. 1. Proposed NIBBCs. (a) Reverse coupling. (b) Forward coupling.

diodes to give zero voltage switching (ZVS) conditions for NIBBCs were used in [3]. However it cannot give bidirectional soft-switching conditions. Two inductor–capacitor (LC) circuits to obtain ZVS conditions were used in [4] and [5]. But it also faces the loss caused by large current ripples. AS NIBBCs use auxiliary circuits, which include active control switches, to obtain zero voltage transition conditions [6]. This type of converter can eliminate most auxiliary circuit losses, but additional control signals and drive circuits are required.

Based on [4] and [5], this letter proposed a new soft-switching NIBBC with coupled inductor. This new dc/dc converter introduces magnetic coupling effect to remove a magnetic core and obtain the adjustment ability of the soft-switching range. Two superiorities of the proposed converter obtained: the efficiency is improved by removing one magnetic core; the introducing of the magnetic coupling effect can increase or decrease the auxiliary current to adjust the soft-switching range.

II. TOPOLOGY AND METHOD

A. Coupling Soft-Switching Method

The soft-switching NIBBC in [4] and [5] can be configured to be a type of converter that uses four capacitors and two inductors. These capacitors employ larger capacitance and also are used as the input and output filter capacitors. This configuration combines auxiliary capacitors and filter capacitors. However, these converters employ three inductor cores that will introduce severe core losses. The proposed NIBBC creates the magnetic coupling effect between two auxiliary inductors, as shown in Fig. 1. The new NIBBC has two types: reverse coupling and forward coupling. Proposed NIBBCs have symmetrical structures, the characteristics of the positive direction (v_a to v_b) will be studied

Manuscript received April 18, 2019; revised May 13, 2019; accepted May 25, 2019. Date of publication May 30, 2019; date of current version September 6, 2019. This work was supported by the National Key R&D Program of China under Grant 2017YFB0103700. (Corresponding author: Xu-Feng Cheng.)

The authors are with the School of Mechanical Engineering, Shanghai Jiao Tong University, Shanghai 200240, China (e-mail: yongzhang1977@sjtu.edu.cn; jdlh2906@sjtu.edu.cn; clyin1965@sjtu.edu.cn).

Color versions of one or more of the figures in this letter are available online at <http://ieeexplore.ieee.org>.

Digital Object Identifier 10.1109/TPEL.2019.2920310

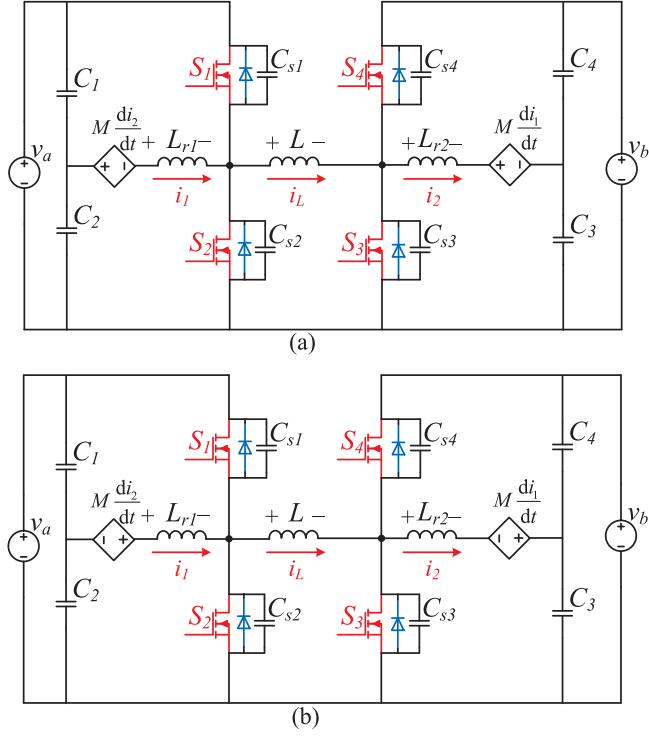


Fig. 2. Equivalent circuits of proposed NIBBCs. (a) Reverse coupling ($-1 < k < 0$). (b) Forward coupling ($0 < k < 1$).

in this letter, and the negative direction (v_b to v_a) has the same characteristics.

Equivalent circuits of two new NIBBCs are shown in Fig. 2. Symbols are defined as: S_n ($n = 1 - 4$) are power transistors; C_n ($n = 1 - 4$) are filter capacitors; C_{sn} ($n = 1 - 4$) are snubber capacitors connected to S_n in parallel; L_{rn} ($n = 1 - 2$) are the auxiliary inductor (a coupled inductor, and $L_{r1} = L_{r2} = L_r$); L is the main inductor; M is the mutual inductance between L_{r1} and L_{r2} , and $M = kL_r$; i_x ($x = 1, 2, L$) are currents across inductors; v_a and v_b are dc voltage sources. If $-1 < k < 1$, then the negative value can represent the reverse coupling, and the positive value can represent the forward coupling. When $k = 0$, the converter is the soft-switching NIBBCs without coupling and is similar to the converter in [4] and [5].

B. Circuit Analysis

As shown in Fig. 3, based on the waveforms of current i_1 , i_2 and i_L , these new NIBBCs have two stages: Stage I ($t_1 - t_4$), and Stage II ($t_4 - t_7$). Then, following equations can be obtained:

1) Stage I: (S_1 and S_3 are OFF and S_2 and S_4 are ON)

$$\begin{cases} k_{L1} = \frac{di_L}{dt} = -\frac{v_b}{L}, & k_{11} = \frac{di_1}{dt} = \frac{v_{c2} + kL_r \frac{di_2}{dt}}{L_r} \\ k_{21} = \frac{di_2}{dt} = \frac{v_b - v_{c3} + kL_r \frac{di_1}{dt}}{L_r}. \end{cases} \quad (1)$$

2) Stage II: (S_1 and S_3 are ON and S_2 and S_4 are OFF)

$$\begin{cases} k_{L2} = \frac{di_L}{dt} = \frac{v_a}{L}, & k_{12} = \frac{di_1}{dt} = \frac{v_{c2} + kL_r \frac{di_2}{dt} - v_a}{L_r} \\ k_{22} = \frac{di_2}{dt} = \frac{kL_r \frac{di_1}{dt} - v_{c3}}{L_r}. \end{cases} \quad (2)$$

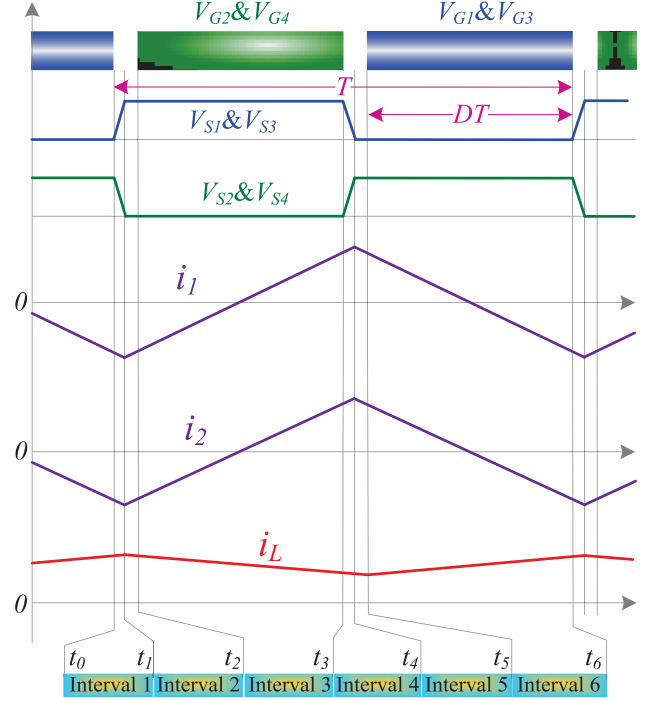


Fig. 3. Waveforms of the proposed NIBBC ($D = 0.5$).

D is the duty cycle of S_1 and S_3 , the relationship of v_a and v_b can be obtained as

$$v_b = v_a D / (1 - D). \quad (3)$$

Then, v_{c2} and v_{c3} can be calculated as

$$v_{c2} = v_{c3} = v_a D. \quad (4)$$

These current differential equations will be

Stage I:

$$\begin{cases} k_{L1} = \frac{di_L}{dt} = -\frac{v_a}{L} \cdot \frac{D}{1-D} \\ k_{11} = \frac{di_1}{dt} = \frac{v_a(1-D+kD)}{L_r(1-k^2)} \cdot \frac{D}{1-D} \\ k_{21} = \frac{di_2}{dt} = \frac{v_a(D+k-kD)}{L_r(1-k^2)} \cdot \frac{D}{1-D}. \end{cases} \quad (5)$$

Stage II:

$$\begin{cases} k_{L2} = \frac{di_L}{dt} = \frac{v_a}{L} \\ k_{12} = \frac{di_1}{dt} = \frac{v_a(D-1-kD)}{L_r(1-k^2)} \\ k_{22} = \frac{di_2}{dt} = \frac{v_a(kD-D-k)}{L_r(1-k^2)}. \end{cases} \quad (6)$$

C. Operating Analysis

Two magnetic coupling NIBBCs have six intervals considering all circuits and devices conduction state in Fig. 3. Fig. 4 gives corresponding converter states of each interval. In these NIBBCs, the current across main inductor L is continuous.

Interval I: This interval begins when S_1 and S_3 are turned OFF. In this interval, snubber capacitors (C_{s1} , C_{s2} , C_{s3} , and C_{s4}) are charging and discharging. Then, the changing rate of drain-source voltages (V_{S1} , V_{S2} , V_{S3} , and V_{S4}) is reduced, the switching-off loss of S_1 and S_3 is reduced.

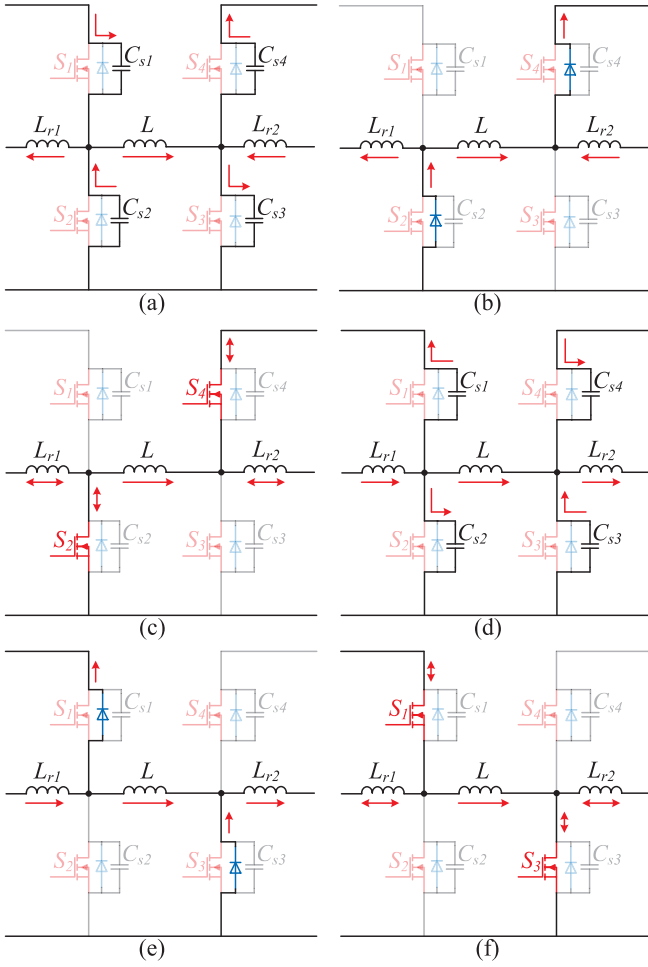


Fig. 4. Component conduction state of every interval. (a) Interval 1. (b) Interval 2. (c) Interval 3. (d) Interval 4. (e) Interval 5. (f) Interval 6.

Interval 2: When antiparallel diodes of S_2 and S_4 are turned ON, this interval starts. In this interval drain-source voltage (V_{S2} and V_{S4}) of S_2 and S_4 are decreasing to 0.

Interval 3: At the beginning of this interval, S_2 and S_4 are turned ON under ZVS conditions. The main inductor L outputs power in this interval.

Interval 4: In this interval, all four switches are OFF. Similar to interval 1, S_2 and S_4 are turned OFF under ZVS conditions.

Interval 5: At t_4 , body diodes of S_1 and S_3 are turned ON, then V_{S1} and V_{S3} decrease to 0.

Interval 6: At t_5 , similar to interval 3, S_1 and S_3 are turned ON under ZVS conditions. In this interval, power is stored in the main inductor L .

III. CHARACTERISTICS

A. Soft-Switching Achieving

In positive direction, the soft-switching condition of all transistors should be considered. i_1 and i_L give ZVS conditions for S_1 and S_2 , and i_2 and i_L give ZVS conditions for S_3 and S_4 . In order to ensure the soft-switching conditions of S_1 and S_3 , the

following equation must be satisfied

$$\begin{cases} i_1(t_5) - i_L(t_5) > 0 \\ i_2(t_5) - i_L(t_5) > 0. \end{cases} \quad (7)$$

Considering the ideal situation (L is large enough to be a current source), the value of i_L will be a constant value in one period, and will be

$$i_L(t_5) = \frac{i_b}{1-D}. \quad (8)$$

i_b is the average current of the load in b -side, and is larger than 0 at the positive direction. For ease of calculation of $i_1(t_5)$ and $i_2(t_5)$, ignoring the dead time, then $i_1(t_5)$ and $i_2(t_5)$ can be obtained as

$$\begin{cases} i_1(t_5) = \frac{v_a DT(1-D+kD)}{2L_r(1-k^2)} \\ i_2(t_5) = \frac{v_a DT(k+D-kD)}{2L_r(1-k^2)}. \end{cases} \quad (9)$$

Substituting (8) and (9) to (7), then

$$\begin{cases} \frac{v_a DT(1-D+kD)}{2L_r(1-k^2)} - \frac{i_b}{1-D} > 0 \\ \frac{v_a DT(k+D-kD)}{2L_r(1-k^2)} - \frac{i_b}{1-D} > 0. \end{cases} \quad (10)$$

Equation (10) can be rewritten as

$$\begin{cases} i_{ss1} = \frac{v_a DT(1-D)(1-D+kD)}{2L_r(1-k^2)} > i_b \\ i_{ss2} = \frac{v_a DT(1-D)(k+D-kD)}{2L_r(1-k^2)} > i_b. \end{cases} \quad (11)$$

Based on the same method, the soft-switching achieving condition of S_2 and S_4 is

$$\begin{cases} i_{ss1} = \frac{v_a DT(1-D)(1-D+kD)}{2L_r(1-k^2)} > -i_b \\ i_{ss2} = \frac{v_a DT(1-D)(k+D-kD)}{2L_r(1-k^2)} > -i_b. \end{cases} \quad (12)$$

Equations (11) and (12) are the soft-switching achieving condition of the proposed NIBBC. The first equations of (11) and (12) limit the soft-switching range of S_1 and S_2 , and the second equations of (11) and (12) limit the soft-switching range of S_3 and S_4 . i_{ss1} and i_{ss2} are maximum values of i_b to ensure soft-switching conditions. i_b cannot be a negative value in the positive direction. Then, parameters, which are satisfied (11), inevitably satisfy (12). The soft-switching range is related to v_a , i_b , k , D , L_r , and T . v_a and i_b represent the input and output influence. k and L_r represent the hardware auxiliary circuit influence. D and T represent the control strategy influence.

To obtain the influence of k and D on the soft-switching range, set $v_a = 100$ V, $L_r = 10$ μ H, and $T = 0.00001$ s, then a map about k , D , and i_{ss1}/i_{ss2} is obtained, as shown in Fig. 5. In Fig. 5, positive values indicate that when i_b is smaller than i_{ss1}/i_{ss2} , S_1/S_3 will obtain soft-switching conditions in positive operation. Negative values indicate that this area has no soft-switching conditions in positive operation.

When k is larger than 0 (forward coupling), i_{ss1} and i_{ss2} are always positive. i_{ss1} and i_{ss2} (maximum values of i_b) are increasing with the increasing of k . i_{ss1} and i_{ss2} increase comparing to the condition without coupling ($k = 0$). Therefore, the forward coupling NIBBC is suitable for high current applications. When k is smaller than 0 (reverse coupling), if D is larger

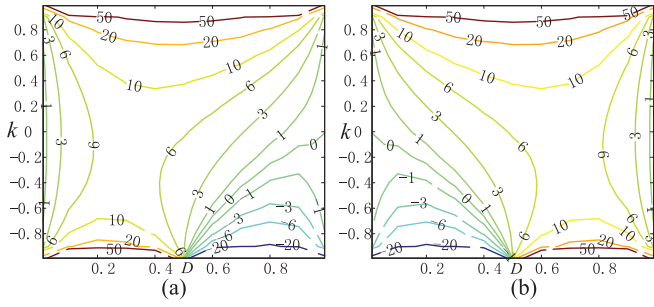


Fig. 5. Map of k and D . (a) i_{ss1} . (b) i_{ss2} .

than 0.5, i_{ss1} will have negative values and is decreasing with the decreasing of k ; if D is smaller than 0.5, i_{ss1} is increasing with the decreasing of k . For i_{ss2} , contrary conclusion is obtained. Therefore, the reverse coupling NIBBC can obtain full soft-switching conditions (all transistors obtain ZVS conditions) around $D = 0.5$. This full soft-switching condition range will reduce with the decreasing of k . In negative value areas of i_{ss1}/i_{ss2} , one transistor (S_1/S_3) will inevitably lose soft-switching conditions.

Overall the forward coupling NIBBC will have a larger soft-switching range than the reverse coupling. Based on these two maps, when k approaches $1/-1$, i_{ss1} and i_{ss2} will approach maximum and minimum values, respectively. In order to keep the NIBBC stable, k cannot be too closed to $1/-1$.

Consider two figures together, if $D = 0.5$, the soft-switching range is largest. If D changes, the full soft-switching range reduces. At this time, If $k > 0$, the maximum load current, which can ensure full soft-switching conditions, will reduce. If $k < 0$, S_1/S_3 will lose soft-switching conditions with the changing of D (increasing or decreasing from 0.5), but the other transistors (S_3/S_1) will obtain the largest value of i_{ss2}/i_{ss1} around $D = 0.75/0.25$.

B. Stress and Loss

The proposed soft-switching NIBBC has the same voltage stress to the traditional NIBBC. Comparing to the inverting buck-boost converter, the voltage stress is reduced. The maximum voltage of S_1 and S_2 is v_a , and the maximum voltage of S_3 and S_4 is v_b . The current stress of this soft-switching NIBBC increases due to the existing of i_1 and i_2 . The maximum current of S_1 and S_2 is $i_L + i_1$, and the maximum voltage of S_3 and S_4 is $i_L + i_2$. When the new NIBBC works under soft-switching conditions, the loss is related to magnetic cores and the maximum value of auxiliary currents (i_1 and i_2). Using coupled inductors, a core is removed, and the core loss and the cost are reduced. The loss will also increase with the increasing of ripples of auxiliary currents (i_1 and i_2).

IV. EXPERIMENT

A. Parameters and Prototype

Parameter design includes two sections: the converter parameter design process and the soft-switching circuit design process. The converter parameter design process gives the switching

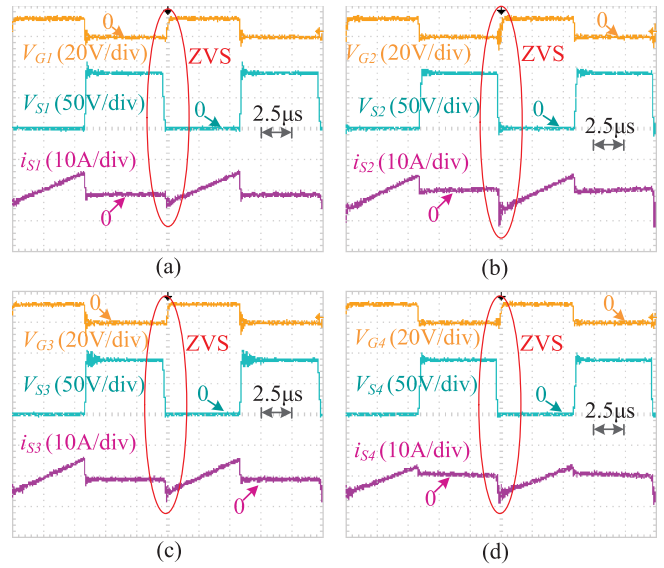


Fig. 6. ZVS waveforms of four transistors. (a) ZVS of S_1 . (b) ZVS of S_2 . (c) ZVS of S_3 . (d) ZVS of S_4 .

frequency and the value of main inductor L based on the working situation of the converter. The soft-switching circuit design process gives the parameter of auxiliary circuit. It can be calculated based on (11) and (12). At first, this section builds an experimental prototype (called prototype I) with reverse coupling to give experimental verifications of soft-switching conditions and the efficiency improvement. Parameters of prototype I are: $L = 295.4 \mu\text{H}$; $L_r = 15.4 \mu\text{H}$; k is around -0.95 ; $D = 0.5$; $v_a = 90 \text{ V}$; $f = 80 \text{ kHz}$; $C_n = 1000 \mu\text{F}$; $C_{sn} = 3.3 \text{ nF}$; and S_n is IRFP4668. A compared ZVS NIBBC without coupling, which is used to verify the efficiency improvement, has same parameters except L_r , and the two L_r in the compared NIBBC have the value about $28 \mu\text{H}$.

B. Experimental Verification

Fig. 6 shows transistor switching waveforms of V_{Gn} , V_{Sn} , and i_{Sn} ($n = 1, 2, 3, 4$). Before the transistor is turned ON, i_{Sn} has a negative value and V_{Sn} is clamped to 0. From these results, ZVS on conditions of all transistors (S_1-S_4) has been achieved. Fig. 7 gives the measuring efficiency result of three converters: the traditional NIBBC without auxiliary circuits, the ZVS NIBBC without coupling (similar to the converter in [4] and [5]), and the proposed NIBBC with coupling. Two ZVS NIBBCs have significant efficiency improving comparing to the traditional NIBBC. The proposed NIBBC has higher efficiency than other two NIBBCs. The idea of this letter, which introduces the magnetic coupling effect and removes a magnetic core, is effective for reducing the core loss.

Then, in order to expand the full soft-switching range, the coupled inductor is redesigned, the value of k is adjusted, and another prototype (called prototype II) is obtained. Its parameters are: L_r is about $19.6 \mu\text{H}$; k is around -0.53 . Other parameters are same to prototype I. Fig. 8 gives measuring efficiency of prototype II in different D . It can be seen that the peak efficiency is largest

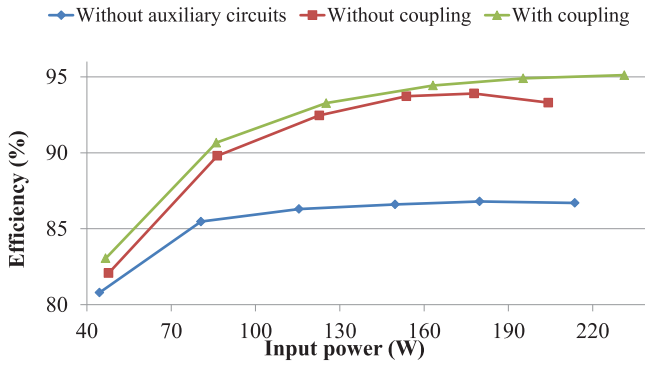


Fig. 7. Comparisons of measured efficiency.

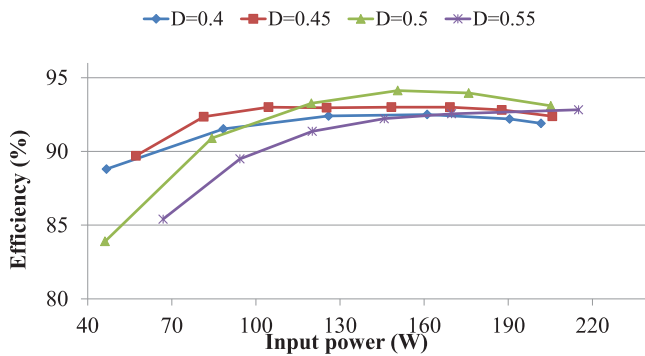


Fig. 8. Measured efficiency of prototype II in different D .

when $D = 0.5$. When D decreases, the soft-switching range narrows, and the light load efficiency increases. Meanwhile the peak of efficiency curves moves to the low-power direction. When D increases, the soft-switching range also narrows, and the output voltage and the voltage stress increase. Meanwhile the efficiency decreases, but the peak of efficiency curves moves to

the high-power direction.

V. CONCLUSION

In this letter, the magnetic coupling effect is introduced to an existing soft-switching NIBBC, and then a new NIBBC is obtained. The coupling coefficient of coupled inductor in new NIBBCs can be adjusted to obtain adjustable soft-switching range. The new converter can obtain efficiency and performance improvement attributes. General analysis and mathematical models of the soft-switching NIBBC with/without coupling are given. Then, through building an experimental prototype, the soft-switching performance and efficiency improvement are verified.

REFERENCES

- [1] Z. Yu, H. Kapels, and K. F. Hoffmann, "A novel control concept for high-efficiency power conversion with the bidirectional non-inverting buck-boost converter," in *Proc. 18th Eur. Conf. Power Electron. Appl.*, Karlsruhe, Germany, 2016, pp. 1–10.
- [2] J. Yu, M. Liu, D. Song, J. Yang, and M. Su, "A soft-switching control for cascaded buck-boost converters without zero-crossing detection," *IEEE Access*, vol. 7, pp. 32522–32536, 2019.
- [3] X. Cheng, Y. Zhang, and C. Yin, "A zero voltage switching topology for non-inverting buck-boost converter," *IEEE Trans. Circuits Syst. II, Express Briefs*, to be published, doi: [10.1109/TCSII.2018.2887105](https://doi.org/10.1109/TCSII.2018.2887105).
- [4] J. Xue and H. Lee, "A 2-MHz 60-W zero-voltage-switching synchronous noninverting buck-boost converter with reduced component values," *IEEE Trans. Circuits Syst. II, Express Briefs*, vol. 62, no. 7, pp. 716–720, Jul. 2015.
- [5] Q. Cheng and H. Lee, "A high-frequency non-isolated ZVS synchronous buck-boost LED driver with fully-integrated dynamic dead-time controlled gate drive," in *Proc. IEEE Appl. Power Electron. Conf. Expo.*, San Antonio, TX, USA, 2018, pp. 419–422.
- [6] L. Cong, J. Liu, and H. Lee, "A high-efficiency low-profile zero-voltage transition synchronous non-inverting buck-boost converter with auxiliary-component sharing," *IEEE Trans. Circuits Syst. I, Reg. Papers*, vol. 66, no. 1, pp. 438–449, Jan. 2019.
- [7] A. Rodriguez, A. Vazquez, M. R. Rogina, and F. Briz, "Synchronous boost converter with high efficiency at light load using QSW-ZVS and SiC MOSFETs," *IEEE Trans. Ind. Electron.*, vol. 65, no. 1, pp. 386–393, Jan. 2018.